J Membrane Biol (2007) 216:129–142
DOI 10.1007/s00232-007-9056-6

Direct and Indirect Effects of Mutations at the Outer Mouth of the Cystic Fibrosis Transmembrane Conductance Regulator Chloride Channel Pore

Jing-Jun Zhou · Mohammad Fatehi · Paul Linsdell

Received: 5 April 2007 / Accepted: 11 June 2007 / Published online: 3 August 2007

Abstract The cystic fibrosis transmembrane conductance regulator (CFTR) Cl^- channel pore is thought to contain multiple binding sites for permeant and impermeant anions. Here, we investigate the effects of mutation of different positively charged residues in the pore on current inhibition by impermeant $Pt(NO_2)_4^{2-}$ and suramin anions. We show that mutations that remove positive charges (K95, R303) influence interactions with intracellular, but not extracellular, $Pt(NO_2)_4^{2-}$ ions, consistent with these residues being situated within the pore inner vestibule. In contrast, mutation of R334, supposedly located in the outer vestibule of the pore, affects block by both extracellular and intracellular $Pt(NO_2)_4^{2-}$. Inhibition by extracellular $Pt(NO_2)_4^{2-}$ requires a positive charge at position 334, consistent with a direct electrostatic interaction resulting in either open channel block or surface charge screening. In contrast, inhibition by intracellular $Pt(NO_2)_4^{2-}$ is weakened in all R334-mutant forms of the channel studied, inconsistent with a direct interaction. Furthermore, mutation of R334 had similar effects on block by intracellular suramin, a large organic molecule that is apparently unable to enter deeply into the channel pore. Mutation of R334 altered interactions between intracellular $Pt(NO_2)_4^{2-}$ and extracellular Cl^- but not those between intracellular $Pt(NO_2)_4^{2-}$ and extracellular $Pt(NO_2)_4^{2-}$. We propose that while the positive charge of R334 interacts directly with extracellular anions, mutation of this residue also alters interactions with intracellular anions by an indirect mechanism, due to mutation-induced conformational changes in the protein that are propagated some distance from the site of the mutation in the outer mouth of the pore.

Keywords Anion permeation · Ion channel · Ion-ion interaction · Open channel block · Surface charge

J.-J. Zhou · M. Fatehi · P. Linsdell (✉)
Department of Physiology and Biophysics, Dalhousie University, 5850 College Street, Halifax, NS, Canada, B3H 1X5
e-mail: paul.linsdell@dal.ca

Present Address:
J.-J. Zhou
Department of Physiology, Fourth Military Medical University, 17 Changle Western Road, 710032, Xi'an, P.R. China

Introduction

Cystic fibrosis (CF) is caused by mutations in the gene encoding the cystic fibrosis transmembrane conductance regulator (CFTR). CFTR is a member of the adenosine triphosphate (ATP)-binding cassette (ABC) family of membrane transport proteins that functions as a cyclic adenosine monophosphate (cAMP)-regulated Cl^- channel in the apical membrane of many different epithelial cell types (Sheppard & Welsh, 1999; Kidd, Kogan & Bear, 2004). While high-resolution crystal structures have been obtained for soluble, intracellular regions of the CFTR protein that are involved in channel gating (Lewis et al., 2004), only low-resolution structural information is currently available for the membrane-spanning region of the protein that presumably forms the pore for transmembrane Cl^- transport (Rosenberg et al., 2004). Consequently, most of what is currently known about the structure and function of the channel pore has come from studying the functional effects of mutations within the transmembrane (TM) domains of the CFTR protein (Liu, Smith & Dawson, 2003; Kidd et al., 2004; Linsdell, 2006). Thus, it has been suggested that, of the 12 TM regions that presumably form the pathway for Cl^- movement across the membrane, TM1, TM5 and TM6 make the most important contributions to the

pore and to the determination of its functional properties (Ge et al., 2004; St. Aubin & Linsdell, 2006).

Recent structure-function studies have highlighted the role of positively charged amino acid side chains in the CFTR channel pore. An arginine residue in TM6, R334, appears to be located in the outer mouth of the pore, where it acts to attract Cl^- ions into the pore from the extracellular solution (Smith et al., 2001). Similarly, the positive charges donated by K95 (in TM1) and R303 (in TM5) act to attract Cl^- ions from the intracellular solution (Linsdell, 2005; St. Aubin & Linsdell, 2006). Current models of the pore place the positive charges of R334 and K95 on the extracellular and intracellular ends, respectively, of a short, narrow section of the pore (Linsdell, 2006), while R303 appears to be located at the cytoplasmic pore mouth (St. Aubin & Linsdell, 2006). Consistent with their location in an internal vestibule in the pore, both K95 and R303 have also been implicated in the formation of binding sites for open channel blockers that enter the pore from its cytoplasmic end (Linsdell, 2005; St. Aubin, Zhou & Linsdell, 2007).

Mutation of R334 has multiple effects on CFTR channel function. The amino acid side chain at this position is thought to be in contact with the lumen of the pore (Cheung & Akabas, 1996; Smith et al., 2001). Mutations that remove the positive charge at this position lead to inward rectification of the current-voltage relationship (Smith et al., 2001; Gong & Linsdell, 2003a), suggesting that this positive charge normally acts to attract Cl^- ions into the outer mouth of the pore by an electrostatic interaction. Mutations at this site also affect block of Cl^- permeation by the high-affinity permeant anion $Au(CN)_2^-$, leading to the suggestion that R334 contributes to a permeant anion binding site (Gong & Linsdell, 2003a). However, all mutations studied, including the charge-conservative R334K, lead to significant weakening of $Au(CN)_2^-$ binding (Gong & Linsdell, 2003a), which is inconsistent with an electrostatic interaction. Furthermore, mutagenesis at R334 has also been associated with weakened binding of intracellularly applied, impermeant anions such as lonidamine (Gong et al., 2002b) and tetranitroplatinate ($Pt[NO_2]_4^{2-}$) (Gong & Linsdell, 2003b), which seems to be inconsistent with the putative location of R334 in the outer mouth of the pore. In addition to weakening $Au(CN)_2^-$ binding inside the pore, all mutations studied at R334 disrupted the interaction between internally applied $Au(CN)_2^-$ ions and extracellular permeant anions, interactions that normally act to relieve channel block and that also contribute to the apparent voltage dependence of block (Gong & Linsdell, 2003a). These findings led our group to suggest that an arginine side chain was absolutely required at position 334 to coordinate repulsive ion-ion interactions within the pore (Gong & Linsdell, 2003a). The effects of mutations at R334 on current-voltage relationship shape are consistent with an electrostatic interaction between external Cl^- ions and the side chain at this position (Smith et al., 2001; Gong & Linsdell, 2003a; *see above*). However, single-channel recording showed that all mutations at this site, including the charge-conservative R334K, lead to a dramatic decrease in the amplitude of unitary currents carried by Cl^- efflux through the pore (Gong & Linsdell, 2004). This suggests that mutation of R334 has both charge-dependent (electrostatic) and charge-independent effects on the rate of Cl^- permeation. It has also been shown that the accessibility of the side chain at this position changes during channel gating, suggesting that channel opening and closing is associated with a conformational change in the pore in the region around R334 (Zhang, Song & McCarty, 2005). The multitude of functional effects associated with mutation of R334 as well as the confusing relationship between these effects and substituted side chain physical properties (Gong & Linsdell, 2003a, 2004) suggest that the role this amino acid residue plays in determining the properties of the pore, while undoubtedly important, is not currently explained.

In recent studies, our group has used the impermeant anion $Pt(NO_2)_4^{2-}$ to probe anion interactions with the CFTR pore (Gong & Linsdell, 2003b; Ge & Linsdell, 2006; Fatehi, St. Aubin & Linsdell, 2007). The results of these studies suggest that both intracellular and extracellular $Pt(NO_2)_4^{2-}$ ions block Cl^- permeation through the pore by interacting with distinct sites in the inner and outer mouths of the pore. However, the molecular bases of these sites are not known. In addition, we have provided evidence that extracellular $Pt(NO_2)_4^{2-}$ ions bind to a site on the CFTR protein that is outside of the pore and that $Pt(NO_2)_4^{2-}$ binding to this site causes a conformational change in the pore that affects its functional properties (Ge & Linsdell, 2006). Again, the location of this putative extra-pore binding site is not known.

In the present work, we identify sites in the pore inner vestibule that are important for interaction with $Pt(NO_2)_4^{2-}$ ions and investigate the role of R334 in determining the interaction between $Pt(NO_2)_4^{2-}$ and the pore. Mutations that neutralize the positive charges associated with K95 and R303 weaken block by intracellular $Pt(NO_2)_4^{2-}$, consistent with an interaction between these residues and blocking anions within the pore inner vestibule. Our results also suggest that mutation of R334 affects binding of internally applied $Pt(NO_2)_4^{2-}$ ions indirectly, probably by causing a conformational change in the channel pore that is sensed at some distance from the site of mutation. In contrast, the effect of R334 mutations on block by externally applied $Pt(NO_2)_4^{2-}$ ions is consistent with an electrostatic interaction, leading us to propose that R334 contributes directly to $Pt(NO_2)_4^{2-}$ interaction with the outer mouth of the pore. In addition, we provide evidence that the binding site for external $Pt(NO_2)_4^{2-}$ ions outside of the pore is independent of R334 and that the mechanism by which $Pt(NO_2)_4^{2-}$ binding

to this site influences the interaction between internally applied blocking ions and the pore is different from the interaction between external Cl^- ions and internal blockers.

Methods

Experiments were carried out on baby hamster kidney (BHK) cells transiently transfected with wild-type or mutant forms of CFTR (Gong et al., 2002a). Macroscopic and single-channel patch-clamp recordings were made from inside-out membrane patches excised from these cells, as described in detail previously (Gong et al., 2002a; Gong & Linsdell, 2003b; St. Aubin & Linsdell, 2006). After patch excision and recording of background currents, CFTR channels were activated by exposure to protein kinase A (PKA) catalytic subunit plus MgATP (1 mM) in the cytoplasmic solution. As in previous studies on these cells (Ge et al., 2004; St. Aubin & Linsdell, 2006), single-channel currents were recorded after weak PKA stimulation (1–5 nM) whereas all macroscopic CFTR currents were recorded after maximal PKA stimulation (~20 nM) and subsequent treatment with sodium pyrophosphate (PPi, 2 mM) to "lock" channels in the open state.

In all experiments, the intracellular (bath) solution contained (mM) 150 NaCl, 2 $MgCl_2$ and 10 *N*-tris(hydroxymethyl)methyl-2-aminoethanesulfonate (TES). The extracellular (pipette) solution contained either the same solution (154 mM Cl^-) or a low-Cl^- solution in which NaCl was replaced by Na gluconate (4 mM Cl^-). In some experiments (*see below*), $K_2Pt(NO_2)_4$ (1–10 mM) was added to the extracellular solution. All experimental solutions were adjusted to pH 7.4 using NaOH. All chemicals were from Sigma-Aldrich (Oakville, Canada) except PKA (Promega, Madison, WI). Intracellular channel blockers were added to the bath solution during the experiment from concentrated stocks made up in bath solution.

Current traces were filtered at 50 Hz (for single-channel currents) or 100 Hz (for macroscopic currents) using an eight-pole Bessel filter, digitized at 250 Hz and analyzed using pCLAMP software (Molecular Devices, Sunnyvale, CA). Single-channel current amplitudes were estimated from all-points amplitude histograms. Macroscopic current-voltage relationships were constructed using depolarizing voltage ramp protocols (Linsdell & Hanrahan, 1996, 1998). Background (leak) currents recorded before addition of PKA were subtracted digitally, leaving uncontaminated CFTR currents (Linsdell & Hanrahan, 1998; Gong & Linsdell, 2003b). Given voltages were corrected for liquid junction potentials calculated using pCLAMP software.

As in previous studies (Gong & Linsdell, 2003b; Ge & Linsdell, 2006), the effects of intracellular $Pt(NO_2)_4^{2-}$ on macroscopic current amplitude were analyzed using the simplest version of the Woodhull (1973) model of voltage-dependent block:

$$I/I_0 = K_d(V)/\{K_d(V) + [B]\} \quad (1)$$

where I is the current amplitude in the presence of $Pt(NO_2)_4^{2-}$, I_0 is the control unblocked current amplitude and $K_d(V)$ is the voltage-dependent dissociation constant, the voltage dependence of which is given by

$$K_d(V) = K_d(0)\exp(-z\delta VF/RT) \quad (2)$$

where $z\delta$ is the effective valence of the blocking ion (actual valence, z, multiplied by fraction of the transmembrane electric field apparently experienced during the blocking reaction) and F, R and T have their usual thermodynamic meanings.

In some cases, mean K_d and $z\delta$ values estimated under different ionic conditions were compared as the ratio between individual values measured with Na gluconate-containing extracellular solutions (Gluc) and the mean value measured with NaCl-containing extracellular solutions (Cl) (Gong & Linsdell, 2003a).

To investigate channel block by external $Pt(NO_2)_4^{2-}$ ions, macroscopic current-voltage relationship shape was compared under different ionic conditions. Initially, macroscopic current amplitudes were normalized to amplitude at −80 mV (I_{REL}). These I_{REL} values obtained with different concentrations of extracellular $Pt(NO_2)_4^{2-}$ were then compared to those obtained in the absence of $Pt(NO_2)_4^{2-}$ ($I_{REL}[0]$). Concentration-inhibition relationships obtained for block by external $Pt(NO_2)_4^{2-}$ were fitted by the following equation:

$$\text{Fractional unblocked current} = 1/(1 + \{[Pt(NO_2)_4^{2-}]/K_d\}^{nH}) \quad (3)$$

where nH is the slope factor or Hill coefficient.

Experiments were carried out at room temperature, 21–24°C. Values are presented as mean ± standard error of the mean (SEM); for graphical presentation, error bars represent ± SEM and, where no error bars are shown, this is smaller than the size of the symbol. Statistical comparisons between groups were carried out using Student's two-tailed *t*-test, with $p < 0.05$ being considered statistically significant.

Results

Neutralization of Positive Charges in the Pore Weakens Block by Intracellular $Pt(NO_2)_4^{2-}$ Ions

$Pt(NO_2)_4^{2-}$ ions block the CFTR Cl^- channel when present on either side of the membrane (Gong & Linsdell, 2003b;

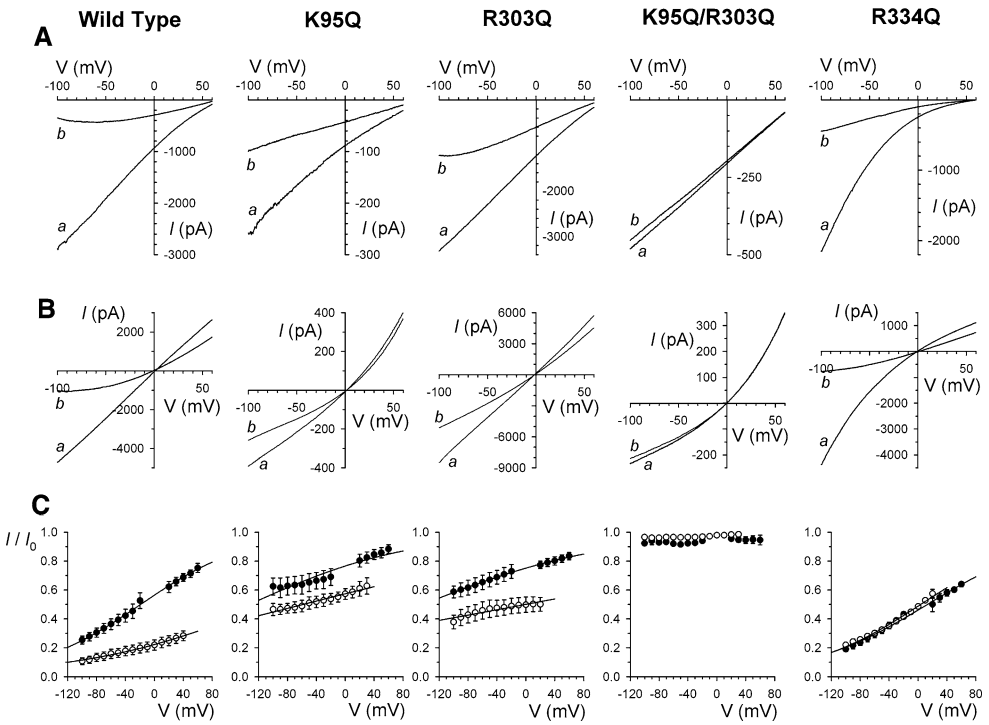

Fig. 1 Removal of positive charges in the pore weakens block by intracellular $Pt(NO_2)_4^{2-}$ ions. **a,b** Example leak-subtracted macroscopic current-voltage relationships recorded from inside-out patches excised from BHK cells transfected with the CFTR variant named above. In **a** the extracellular solution contained 4 mM Cl^-, while in **b** it contained 154 mM Cl^-. In each case currents were recorded following maximal channel stimulation with PKA and PPi, both before (**a**) and after (**b**) addition of 300 μM $K_2Pt(NO_2)_4$ to the intracellular solution, to show the inhibitory effects of $Pt(NO_2)_4^{2-}$. (**c**) Mean fraction of control current remaining (I/I_0) at different voltages following addition of this concentration of $Pt(NO_2)_4^{2-}$, with both 4 mM (◯) and 154 mM(●) extracellular Cl^-. Mean of data from three to eight patches. Fitted lines are to equation 1, with the following parameters: wild type 4 mM external Cl^-, $K_d(0) = 85.8$ μM, $z\delta = -0.201$; wild type 154 mM external Cl^-, $K_d(0) = 387$ μM, $z\delta = -0.344$; K95Q 4 mM external Cl^-, $K_d(0) = 403$ μM, $z\delta = -0.130$; K95Q 154 mM external Cl^-, $K_d(0) = 978$ μM, $z\delta = -0.227$; R303Q 4 mM external Cl^-, $K_d(0) = 300$ μM, $z\delta = -0.096$; R303Q 154 mM external Cl^-, $K_d(0) = 904$ μM, $z\delta = -0.197$; R334Q 4 mM external Cl^-, $K_d(0) = 286$ μM, $z\delta = -0.330$; R334Q 154 mM external Cl^-, $K_d(0) = 256$ μM, $z\delta = -0.307$. Because block was so weak at this concentration, data for the K95Q/R303Q double mutant were not fitted

Ge & Linsdell, 2006), most likely by interacting with different sites (Fatehi et al., 2007). While altered $Pt(NO_2)_4^{2-}$ block has been reported in some CFTR pore mutants (Gong & Linsdell, 2003b), the molecular basis of $Pt(NO_2)_4^{2-}$ block is not clear. Figure 1 shows the effect of point mutations that neutralize important positive charges in the pore (K95, R303, R334) on block by intracellular $Pt(NO_2)_4^{2-}$ ions. Whether studied under conditions of low (Fig. 1a) or high (Fig. 1b) extracellular Cl^- concentration, $Pt(NO_2)_4^{2-}$ block is significantly weakened in both K95Q and R303Q (Figs. 1c, 2). This is consistent with the proposed location of these two residues within the pore inner vestibule and their involvement in attracting intracellular Cl^- ions into the pore by an electrostatic mechanism (Linsdell, 2005; St. Aubin & Linsdell, 2006) and in contributing to binding sites for intracellular open channel blockers (St. Aubin et al., 2007). Furthermore, a double mutant in which both of these positive charges are neutralized (K95Q/R303Q) generated currents that were almost completely insensitive to the blocking effects of $Pt(NO_2)_4^{2-}$ (Fig. 1), consistent with the overall channel-blocking effects of $Pt(NO_2)_4^{2-}$ ions being the result of interactions with both of these purportedly independent sites (St. Aubin et al., 2007). In spite of the weakened blocking effects of intracellular $Pt(NO_2)_4^{2-}$ seen in both K95Q and R303Q, block of each of these two mutants was still significantly weakened by extracellular Cl^- ions (Figs. 1c, 2).

Neutralization of a third pore-forming positive charge, in the R334Q mutant, was also associated with significant weakening of the blocking effects of internal $Pt(NO_2)_4^{2-}$ (Figs. 1, 2). This is consistent with previously reported weakening of intracellular $Pt(NO_2)_4^{2-}$ block in R334C (Gong & Linsdell, 2003b). However, unlike K95Q and R303Q, the R334Q mutant weakened $Pt(NO_2)_4^{2-}$ block at low, but not high, extracellular Cl^- concentration (Fig. 2). This difference likely results from the fact that the R334Q mutation also apparently removes the sensitivity of block to extracellular Cl^- concentration (Figs. 1c, 2).

As described above, weakened block by intracellular $Pt(NO_2)_4^{2-}$ ions in K95Q and R303Q is consistent with

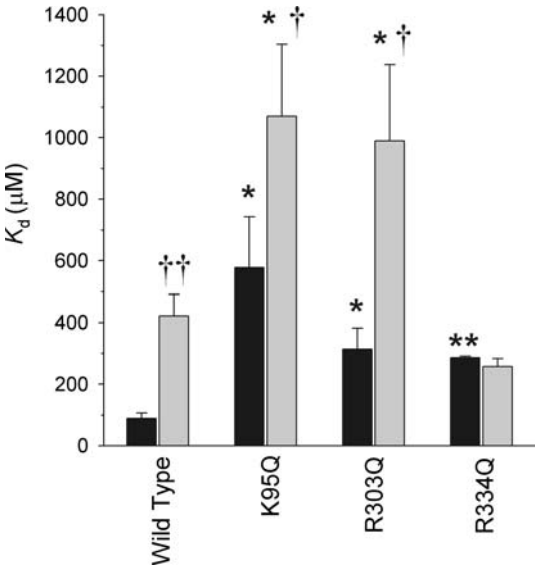

Fig. 2 Effect of neutralization of different positive charges on block by intracellular $Pt(NO_2)_4^{2-}$. Mean K_d (at 0 m*V*) was estimated by fitting data from individual patches such as those shown in Figure 1 by equation 1. Data shown for both 4 mM extracellular Cl^- (*black bars*) and 154 mM extracellular Cl^- (*gray bars*). Mean of data from three to eight patches. Asterisks indicate a significant difference from the corresponding value in wild type ($*p < 0.05$, $**p < 0.001$), while daggers indicate a significant difference from the same channel variant at 4 mM Cl^- ($^{\dagger}p < 0.05$, $^{\dagger\dagger}p < 0.001$)

current models of the pore that place these two positively charged amino acid residues within the pore inner vestibule. In contrast, R334 is thought to reside in the outer vestibule of the pore (Smith et al., 2001; Linsdell, 2006), and the mechanism by which neutralization of this residue would weaken the blocking effects of an intracellularly applied, impermeant blocker is less obvious.

Characterization of the Effect of Mutations at R334 on Block by Intracellular $Pt(NO_2)_4^{2-}$ Ions

To investigate further the role of R334 in controlling block by intracellular $Pt(NO_2)_4^{2-}$ ions, we investigated the effects of other substitutions at this position. Figure 3 shows the blocking effects of internally applied $Pt(NO_2)_4^{2-}$ in six different channel mutants (R334C, R334E, R334H, R334K, R334L, R334Q) under conditions of both low (Fig. 3a) and high (Fig. 3b) extracellular Cl^- concentration. The overall blocking effects of $Pt(NO_2)_4^{2-}$ on these different mutants are compared to wild type in Figure 4. All mutations at R334 were associated with weakening of $Pt(NO_2)_4^{2-}$ block under conditions of low extracellular Cl^-. All mutants also show a diminished effect of extracellular Cl^- ions on the strength of block. These effects are seen more clearly from estimates of the apparent blocker K_d shown in Figure 5. With low extracellular Cl^- concentrations, the K_d for $Pt(NO_2)_4^{2-}$ block (at 0 mV) was significantly increased in all six R334 mutants studied (Fig. 5a), although it is clear that R334C and R334E had far greater effects on K_d compared to other amino acid substitutions. With elevated extracellular Cl^-, the $K_d(0)$ was significantly increased only in R334C and R334E; not significantly altered in R334K, R334L and R334Q; and significantly decreased in R334H (Fig. 5b). Comparison of the K_d estimated under different extracellular Cl^- concentrations (Fig. 5c) revealed that all six mutants studied had a significantly weakened (in fact, practically abolished) sensitivity of block to extracellular Cl^- ions. These R334 mutations also exhibited a weakened sensitivity of blocker voltage dependence (quantified as $-z\delta$, Fig. 5) to external Cl^- concentration (Fig. 5c), although because of the small magnitude of this effect only R334C, R334H and R334Q reached a level of statistical significance (Fig. 5c).

Mutation of R334 Affects Block by Intracellular Suramin

The effects of R334 mutations on block by intracellular $Pt(NO_2)_4^{2-}$ described above suggest that this residue influences both the affinity and extracellular Cl^- dependence of block. This is somewhat surprising given (1) the proposed location of R334 in the pore outer vestibule (Smith et al., 2001; Linsdell, 2006), (2) the impermeability of $Pt(NO_2)_4^{2-}$ in CFTR (Gong & Linsdell, 2003b) and its supposed restriction to binding sites on the same side of the membrane as that to which it is applied (Fatehi et al., 2007) and (3) possible localization of $Pt(NO_2)_4^{2-}$ binding sites in the pore inner vestibule, around the locations of K95 and R303 (Figs. 1, 2). This suggests that either $Pt(NO_2)_4^{2-}$ is able to pass most of the way through the pore, close enough to R334 in the outer vestibule to sense the nature of the amino acid side chain at this position, or the effects of mutations at R334 on $Pt(NO_2)_4^{2-}$ block are indirect, perhaps caused by mutation-induced changes in the conformation of the pore inner vestibule. To try to separate these possibilities, we sought to investigate the effects of an intracellular open channel blocker that could not approach close to the pore outer vestibule. We chose suramin, a large organic anion that blocks the channel, apparently due predominantly to interactions with R303 at the cytoplasmic mouth of the pore (St. Aubin et al., 2007). Since block by intracellular suramin is insensitive even to mutations at K95, located relatively deep in the pore inner vestibule (Linsdell, 2005; St. Aubin et al., 2007), we believe that suramin does not enter far into the pore from its cytoplasmic end and is therefore highly unlikely to be able to sense directly the nature of amino acid residues in the outer pore mouth.

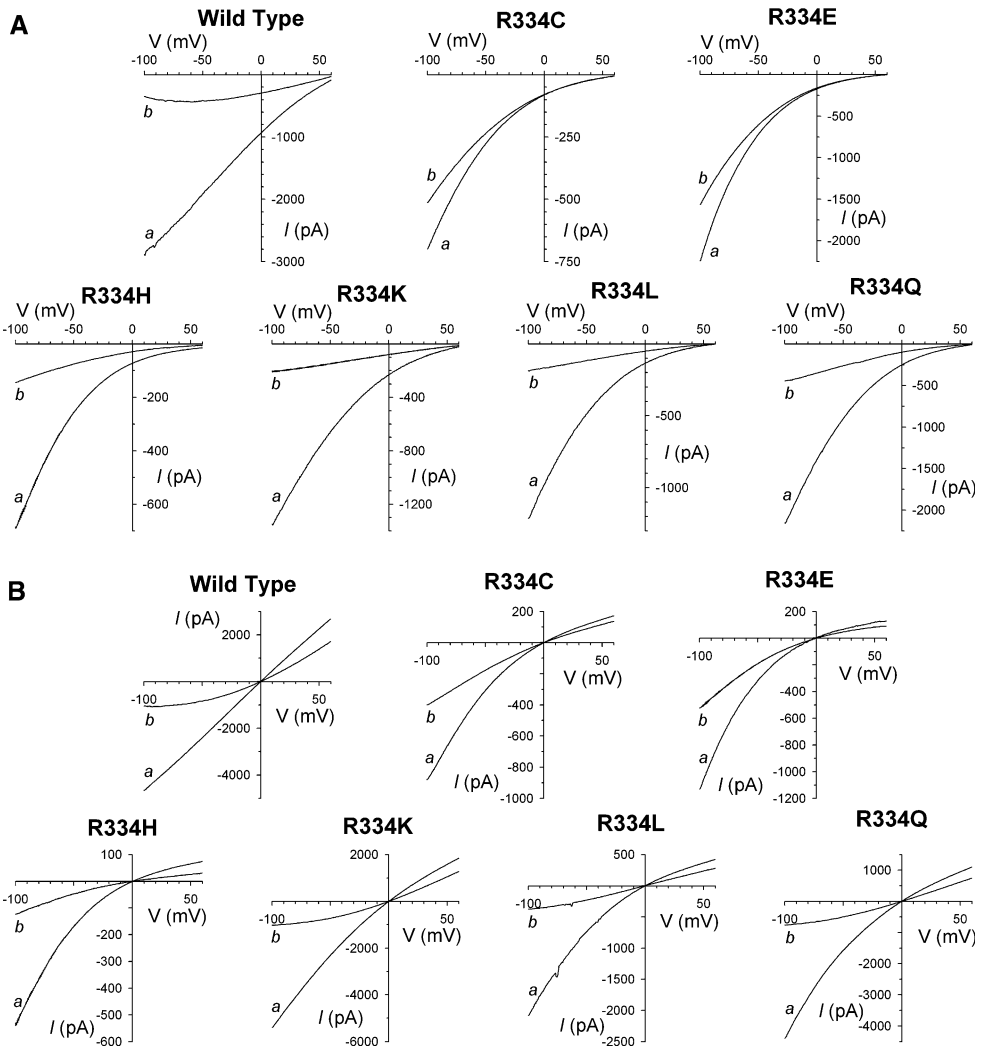

Fig. 3 Intracellular $Pt(NO_2)_4^{2-}$ block of different R334 mutants. Example leak-subtracted macroscopic current-voltage relationships for the named channel variants before (**a**) and after (**b**) addition of of 300 μM $K_2Pt(NO_2)_4$ to the intracellular solution, either with 4 mM (**a**) or 154 mM (**b**) extracellular Cl

The effects of intracellular suramin on wild-type and R334-mutant forms of CFTR are compared in Figure 6. Because suramin block is insensitive to extracellular Cl^- concentration (St. Aubin et al., 2007), these experiments were carried out only using low external Cl^- conditions. Comparison of the mean K_d estimated for suramin (at 0 m*V*) shows that R334C, R334E, R334K, R334L and R334Q were all associated with weakened suramin block, with only R334H failing to significantly affect suramin block (Fig. 7). Suramin block was particularly weakened in R334C and R334E (Figs. 6, 7) such that the profiles of mutation effects on block by internal $Pt(NO_2)_4^{2-}$ and suramin are very similar.

Mutation of R334 Does not Affect Interactions between Intracellular and Extracellular $Pt(NO_2)_4^{2-}$ Ions

Block of wild-type CFTR by intracellular $Pt(NO_2)_4^{2-}$ is significantly weakened by $Pt(NO_2)_4^{2-}$ ions present in the extracellular solution, an effect which is apparently independent of the ability of external $Pt(NO_2)_4^{2-}$ ions directly to inhibit Cl^- permeation (Ge & Linsdell, 2006). Since mutation of R334 affected interactions between intracellular $Pt(NO_2)_4^{2-}$ and extracellular Cl^- (Figs. 1c, 2, 5c), we wondered if this residue was also involved in interactions between internal and external $Pt(NO_2)_4^{2-}$ ions. As shown in Figure 8, although block by internal $Pt(NO_2)_4^{2-}$ is significantly weakened in R334Q, this blocking effect is still sensitive to the presence of $Pt(NO_2)_4^{2-}$ ions in the extracellular solution. In wild type, addition of 8 mM $Pt(NO_2)_4^{2-}$ to the extracellular solution increased mean $K_d(0)$ for intracellular $Pt(NO_2)_4^{2-}$ approximately 2.7-fold without significantly altering $-z\delta$, while in R334Q this concentration of extracellular $Pt(NO_2)_4^{2-}$ increased mean $K_d(0)$ 2.5-fold, again with no significant change in $-z\delta$ (Fig. 8c). Thus, the R334Q mutation practically abolishes the dependence of intracellular $Pt(NO_2)_4^{2-}$ block on external Cl^- (Figs. 1c, 2, 5c) without significantly altering its dependence on external $Pt(NO_2)_4^{2-}$ (Fig. 8).

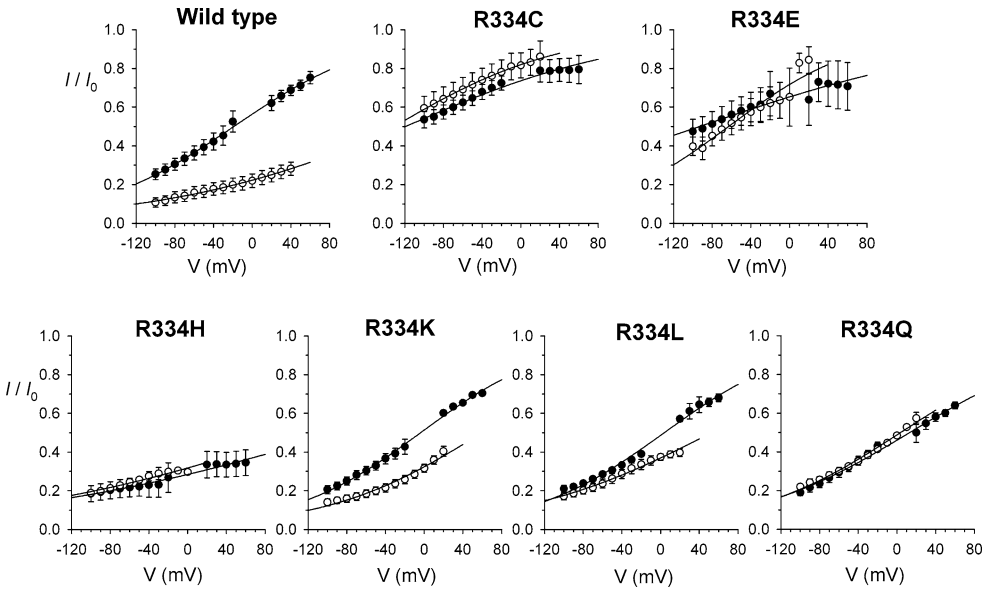

Fig. 4 Effect of different substitutions of R334 on block by intracellular $Pt(NO_2)_4^{2-}$. Mean fraction of control current remaining (I/I_0) at different voltages following addition of 300 μM $K_2Pt(NO_2)_4^{2-}$ to the intracellular solution, with both 4 mM (◯) and 154 mM (●) extracellular Cl^-. Mean of data from three to eight patches. Fitted lines are to equation 1 as described in Figure 1 for wild type and R334Q and with the following parameters for other channel variants: R334C 4 mM external Cl^-, $K_d(0)$ = 1362 μM, zδ = −0.295; R334C 154 mM external Cl^-, $K_d(0)$ = 836 μM, zδ = −0.219; R334E 4 mM external Cl^-, $K_d(0)$ = 759 μM, zδ = −0.376; R334E 154 mM external Cl^-, $K_d(0)$ = 564 μM, zδ = −0.173; R334H 4 mM external Cl^-, $K_d(0)$ = 140 μM, zδ = −0.166; R334H 154 mM external Cl^-, $K_d(0)$ = 119 μM, zδ = −0.149; R334K 4 mM external Cl^-, $K_d(0)$ = 143 μM, zδ = −0.314; R334K 154 mM external Cl^-, $K_d(0)$ = 317 μM, zδ = −0.374; R334L 4 mM external Cl^-, $K_d(0)$ = 176 μM, zδ = −0.258; R334L 154 mM external Cl^-, $K_d(0)$ = 284 μM, zδ = −0.366

Characterization of the Effect of Mutations at R334 on Block by Extracellular $Pt(NO_2)_4^{2-}$ Ions

Block of CFTR by external $Pt(NO_2)_4^{2-}$ ions is most apparent at the single-channel level (Fig. 9). As described previously (Ge & Linsdell, 2006; Fatehi et al., 2007), inclusion of $Pt(NO_2)_4^{2-}$ in the pipette solution led to a strongly voltage-dependent reduction in unitary current amplitude (Fig. 9). Unfortunately, single-channel recording cannot be used to investigate blocker effects on the R334 mutants described above since each of these mutants shows very low unitary conductance even in the absence of blocking ions (Gong & Linsdell, 2004). Blockers can be added to the extracellular solution during whole-cell recording; however, this technique sometimes gives different results in CFTR when compared to measurements of single-channel current amplitude, perhaps because the blocker affects both Cl^- conductance and channel gating (*see* Fatehi et al., 2007). In order to compare the blocking effects of external $Pt(NO_2)_4^{2-}$ ions in R334-mutant forms of CFTR, we therefore used a somewhat indirect measure of blocker potency that relies on the strong voltage dependence of block we observe in wild type (Fig. 9).

We estimated the relative potency of external $Pt(NO_2)_4^{2-}$ block by analysis of the shape of the macroscopic current-voltage relationship (Fig. 10). As shown in Figure 10a, inclusion of increasing concentrations of $Pt(NO_2)_4^{2-}$ in the pipette solution led to increasing inward rectification of the current-voltage relationship in wild-type CFTR. Since these current-voltage relationships were recorded after the channel was locked open with PPi, any effect on channel gating should be removed and the macroscopic current-voltage relationship should have the same form as the unitary current-voltage relationship recorded in the absence of PPi. In fact, in no case was macroscopic current-voltage relationship shape significantly changed by addition of PPi. The inward rectification induced by $Pt(NO_2)_4^{2-}$ could reflect one of two effects. First, it may be that binding of $Pt(NO_2)_4^{2-}$ within the pore outer vestibule causes a strongly voltage-dependent open channel block of Cl^- permeation. Second, $Pt(NO_2)_4^{2-}$ could act by screening important surface charges (Green & Andersen, 1991), leading to loss of electrostatic attraction on external Cl^- ions that is important for Cl^- influx at positive voltages (Smith et al., 2001). While mechanistically important (*see* Discussion), this distinction makes no difference to the validity of the analysis.

Since external $Pt(NO_2)_4^{2-}$, even at concentrations as high as 10 mM, has no significant effect on unitary current amplitude at hyperpolarized voltages (Fig. 9), we compared the shape of macroscopic current-voltage relationships in the presence of different concentrations of

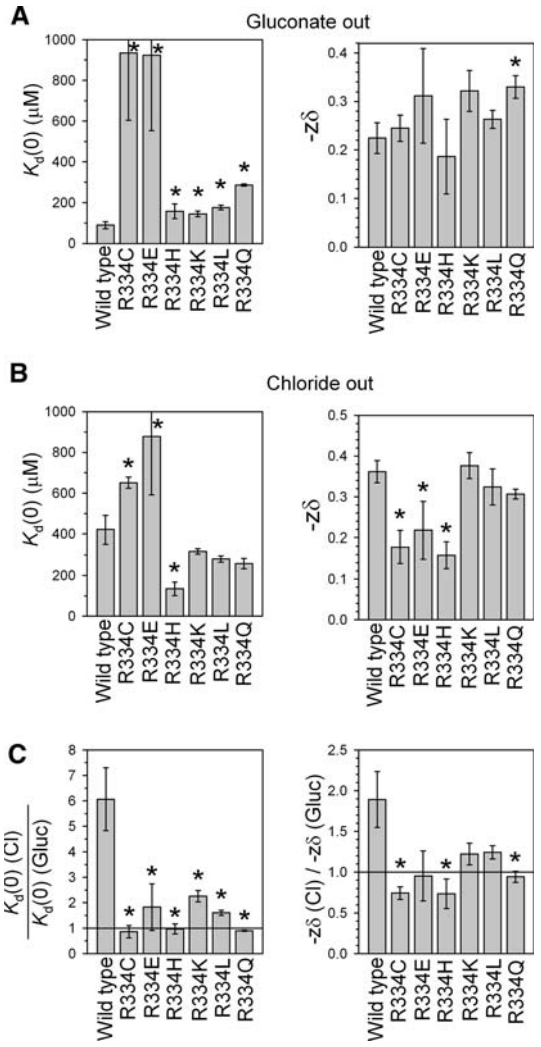

Fig. 5 Effect of mutations at R334 on the properties of block by intracellular $Pt(NO_2)_4^{2-}$. Mean $K_d(0)$ and $-z\delta$ calculated from fits to data from individual patches for different channel variants, with 4 mM (**a**) and 154 mM (**b**) extracellular Cl^-. **c** The effect of changing the extracellular Cl^- concentration from 4 to 154 mM is expressed as the ratio of either $K_d(0)$ (*left*) or $-z\delta$ (*right*) under these different ionic conditions. Asterisks indicate a significant difference from wild type ($p < 0.05$). Mean of data from three to eight patches in each case

extracellular $Pt(NO_2)_4^{2-}$ by normalizing current amplitude at the hyperpolarized extreme of the voltage range studied, –80 m*V* (Fig. 10b). It can be seen that the mean normalized current-voltage relationships produced in this way have a very similar form to the unitary current-voltage relationships recorded under the same ionic conditions (Fig. 9c). Relative current in the presence of different concentrations of $Pt(NO_2)_4^{2-}$ is shown as a fraction of relative control current amplitude at the same voltage in Figure 10c; these relationships are analogous to the fractional unitary current-voltage relationships of Figure 9d. To show the close agreement between direct single-channel analysis and indirect macroscopic current-voltage relationship analysis, mean concentration-inhibition curves constructed by these two methods at +80 m*V* are compared in Figure 10d; as described in the legend to Figure 10, fits to these sets of data give very similar apparent K_d values for external $Pt(NO_2)_4^{2-}$ of 2.85 mM from single-channel currents (without PPi) and 2.73 mM from macroscopic currents (with PPi).

We then applied this same analysis to macroscopic current-voltage relationships obtained from pore-mutant forms of CFTR (Fig. 11). One potential caveat in doing so is that we do not have independent confirmation that external $Pt(NO_2)_4^{2-}$ does not block these mutants at strongly hyperpolarized voltages, which is an assumption of the analysis. However, we considered that these mutations would be more likely to alter the apparent affinity of block at depolarized voltages than to cause the appearance of block at hyperpolarized voltages. Example macroscopic current-voltage relationships for wild type and each R334 mutant studied, as well as mutations that neutralize positive charges involved in binding of intracellular $Pt(NO_2)_4^{2-}$ (K95Q, R303Q), are compared in Figure 11a. In each panel, two current-voltage relationships, recorded from different patches and normalized to current amplitude at –80 m*V*, are shown, representing control conditions (no $Pt[NO_2]_4^{2-}$) and 10 mM extracellular $Pt(NO_2)_4^{2-}$. As described previously (Smith et al., 2001; Gong & Linsdell, 2003a), mutagenesis of R334 led to strong inward rectification even under control conditions. However, it can be seen that for all R334 mutations except the charge-conservative R334K, current-voltage relationship shape was not strongly altered by the presence of $Pt(NO_2)_4^{2-}$ in the extracellular solution. Both K95Q and R303Q are associated with outward rectification under control conditions; this rectification was apparently weakened in the presence of extracellular $Pt(NO_2)_4^{2-}$, most likely due to voltage-dependent current inhibition, which was most prominent at depolarized voltages. The mean effects of 10 mM $Pt(NO_2)_4^{2-}$ in each channel variant, analyzed as described above for wild type (Fig. 10c), are illustrated in Figure 11b (for R334 mutants) and 11c (for K95Q and R303Q). Considering only the data at +80 m*V* (Fig. 11d), where block of wild-type CFTR is strongest (Figs. 9, 10), the blocking effects of $Pt(NO_2)_4^{2-}$ are slightly (but significantly) weakened in K95Q, R303Q and R334K ($p < 0.05$) but practically abolished in all other R334 mutants ($p < 0.0005$). In fact, only wild type, R334K, K95Q and R303Q – those mutants that retain a positive charge at position 334 – were significantly affected by 10 mM $Pt(NO_2)_4^{2-}$ according to this analysis (as illustrated by the daggers in Fig. 11d, $p < 0.001$), whereas all mutants associated with removal of the positive charge at R334 showed no significant differences in the absence or presence of external $Pt(NO_2)_4^{2-}$ ($p > 0.15$).

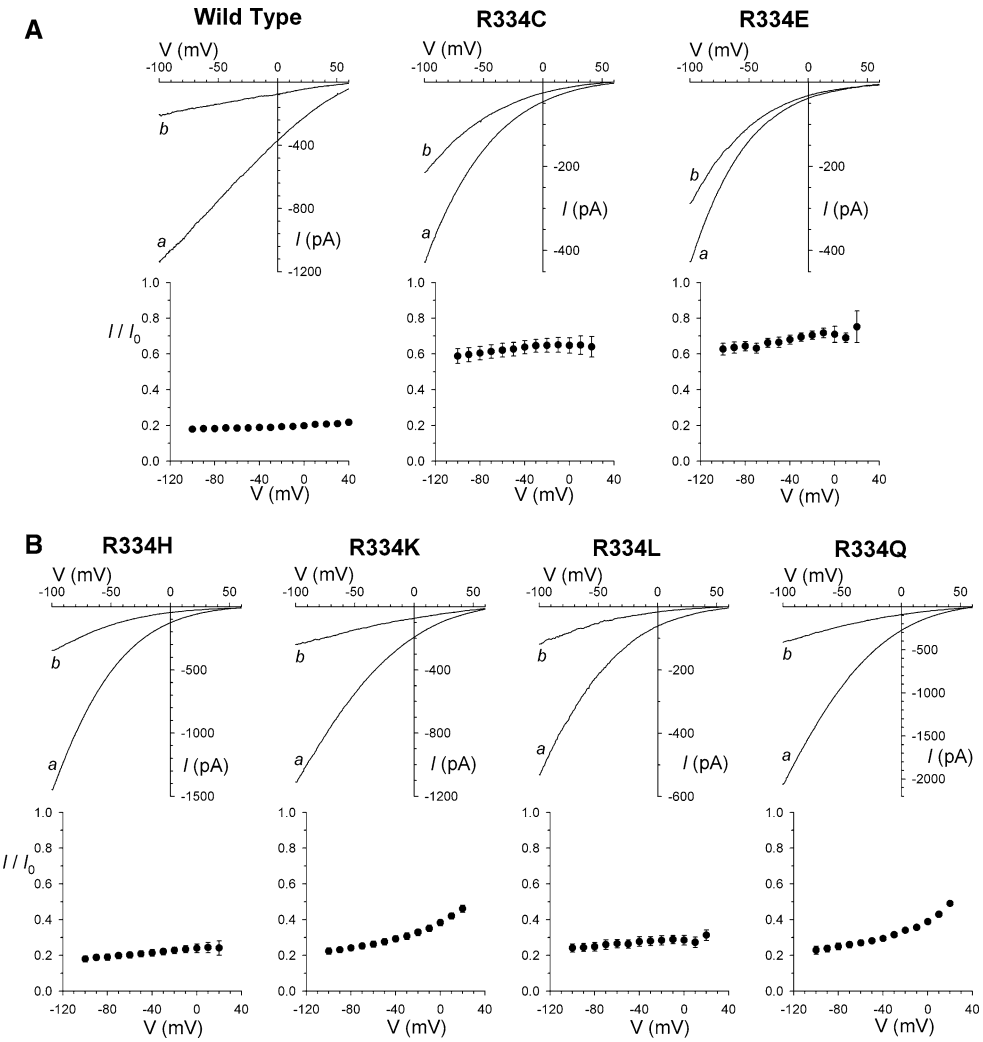

Fig. 6 Block of different R334 mutants by intracellular suramin. For each channel variant named is an example leak-subtracted macroscopic current-voltage relationship recorded before (**a**) and after (**b**) addition of 10 μM suramin to the intracellular solution. Beneath each current-voltage relationship is the corresponding mean fraction of control current remaining (I/I_0) at different voltages following addition of this concentration of suramin. These plots represent mean data from four to seven patches. Fitted lines are to equation 1 with the following parameters: wild type, $K_d(0)$ = 2.51 μM, zδ = −0.042; R334C, $K_d(0)$ = 18.5 μM, zδ = −0.056; R334E, $K_d(0)$ = 25.0 μM, zδ = −0.107; R334H, $K_d(0)$ = 3.10 μM, zδ = −0.085; R334K, $K_d(0)$ = 6.31 μM, zδ = −0.232; R334L, $K_d(0)$ = 4.08 μM, zδ = −0.061; R334Q, $K_d(0)$ = 6.64 μM, zδ = −0.239

Discussion

Previous studies have suggested that $Pt(NO_2)_4^{2-}$ ions applied to the intracellular or extracellular solution block Cl^- permeation in CFTR by binding to distinct sites in the pore (Ge & Linsdell, 2006; Fatehi et al., 2007). Our present results suggest that block by intracellular $Pt(NO_2)_4^{2-}$ involves interactions with positively charged amino acid side chains in the wide inner vestibule of the pore since mutations that remove these positive charges (K95Q, R303Q) lead to significant weakening of $Pt(NO_2)_4^{2-}$ block (Figs. 1, 2). Furthermore, removal of both positive charges (in the K95Q/R303Q double mutant) gave rise to a channel that was almost completely resistant to the blocking effects of internal $Pt(NO_2)_4^{2-}$ (Fig. 1), suggesting that both positive charges contribute to $Pt(NO_2)_4^{2-}$ binding in the pore inner vestibule. Given the proposed locations of these two positively charged amino acids – K95 is thought to be located in a central region, on the internal side of a narrow pore region (Linsdell, 2005, 2006), whereas R303 is likely located at the cytoplasmic mouth of the pore (St. Aubin & Linsdell, 2006; St. Aubin et al., 2007) – we suggest that $Pt(NO_2)_4^{2-}$ ions block the channel at either of two sites involving these two positive charges. This is consistent with the idea that K95 and R303 contribute to anion binding sites that are independent of one another (St. Aubin et al., 2007). Alternatively, these two positively charged residues may act by attracting $Pt(NO_2)_4^{2-}$ ions into the inner vestibule by an electrostatic mechanism, in the same way as has been proposed for Cl^- ions (Linsdell, 2005; St. Aubin & Linsdell, 2006). Since other pore-lining residues contributing to $Pt(NO_2)_4^{2-}$ binding have not been described, this would mean that the $Pt(NO_2)_4^{2-}$ binding site(s) remains to be identified.

Block by intracellular $Pt(NO_2)_4^{2-}$ ions was also significantly weakened by mutation of another positively charged pore-forming residue, R334 (Figs. 1–5), consistent with previous results showing significant weakening of the blocking effects of intracellular $Au(CN)_2^-$ ions in these mutants (Gong & Linsdell, 2003a). However, in contrast

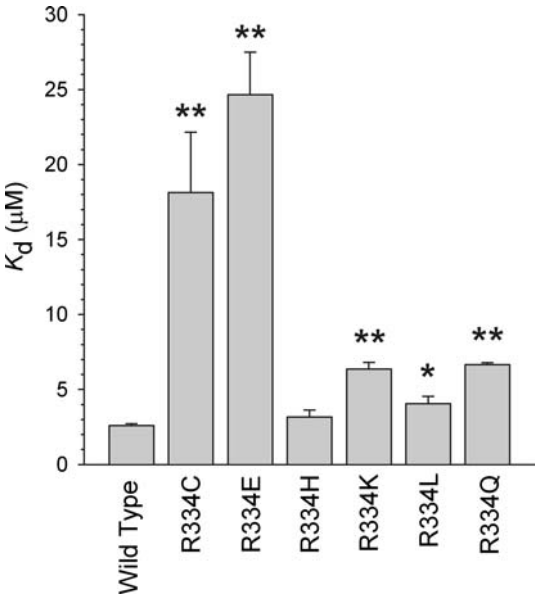

Fig. 7 Effect of different substitutions of R334 on block by intracellular suramin. Mean K_d (at 0 m*V*) was estimated by fitting data from individual patches such as those shown in Figure 6 by equation 1. Mean of data from four to seven patches. Asterisks indicate a significant difference from wild type (*$p < 0.01$, **$p < 0.001$)

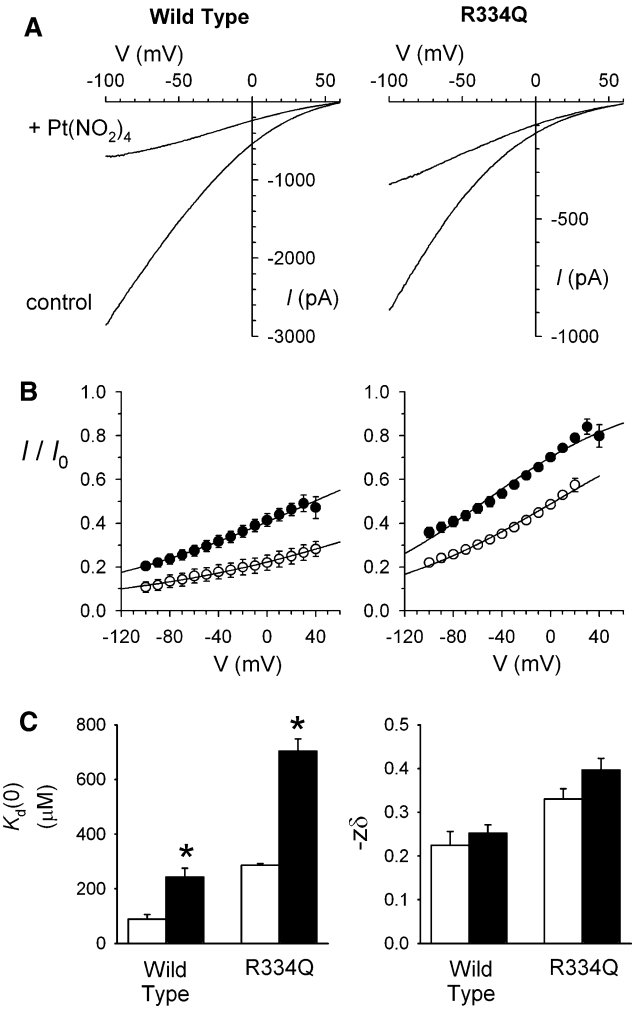

Fig. 8 Extracellular $Pt(NO_2)_4^{2-}$ modifies block by intracellular $Pt(NO_2)_4^{2-}$ following neutralization of the positive charge at R334. **a** Example leak-subtracted macroscopic current-voltage relationships recorded with 8 mM $K_2Pt(NO_2)_4^{2-}$ present in the extracellular solution for wild type (*left*) and R334Q (*right*), recorded before (control) and after (+ $Pt[NO_2]_4$) addition of 300 μM $K_2Pt(NO_2)_4$ to the intracellular solution. **b** Mean fraction of control current remaining (I/I_0) at different voltages following addition of $Pt(NO_2)_4^{2-}$ under these ionic conditions (●) is compared with the effects of the same concentration of $Pt(NO_2)_4^{2-}$ measured in the absence of extracellular $Pt(NO_2)_4^{2}$ (○; same data as in Fig. 1c). Mean of data from three to eight patches. Fitted lines are to equation 1 with the following parameters: wild type (○), $K_d(0)$ = 85.8 μM, -zδ = 0.201; wild type (●), $K_d(0)$ = 205 μM, -zδ = 0.248; R334Q (○), $K_d(0)$ = 286 μM, -zδ = 0.330; R334Q (●), $K_d(0)$ = 704 μM, -zδ = 0.401. **c** Mean $K_d(0)$ and –zδ calculated under these conditions, without extracellular $Pt(NO_2)_4^{2-}$ (*white bars*) and with 8 mM $Pt(NO_2)_4^{2-}$ (*black bars*). Mean of data from four to seven patches. Asterisks indicate a significant difference from zero extracellular $Pt(NO_2)_4$ conditions ($p < 0.005$)

with our previous suggestion that intracellular $Au(CN)_2^-$ blocks the channel by interacting directly with R334, several reasons prompt us to suggest that $Pt(NO_2)_4^{2-}$ does not interact directly with the arginine side chain at this position. First, the proposed location of the R334 residue, in the outer mouth of the pore (Smith et al., 2001; Liu et al., 2003; Linsdell, 2006) appears inconsistent with interaction with an impermeant anion applied to the cytoplasmic mouth of the pore. Second, $Pt(NO_2)_4^{2-}$ block is significantly weakened in all of the six R334-mutated variants studied, including the charge-conservative R334K (Fig. 5a). Thus, while $Pt(NO_2)_4^{2-}$ block is particularly weak in R334C and R334E (Figs. 3–5), there is no strong correlation between the apparent affinity of $Pt(NO_2)_4^{2-}$ block and the nature of the side chain present at position 334. Third, mutations at R334 had qualitatively similar effects on block by intracellular suramin (Figs. 6, 7) as they did on block by $Pt(NO_2)_4^{2-}$. We chose to investigate suramin block since this substance appears to be able to enter only into the most superficial parts of the pore inner vestibule when applied to the cytoplasmic solution (St. Aubin et al., 2007); in fact, it appears that suramin does not enter deeply enough into the pore to experience electrostatic interactions with K95 (St. Aubin et al., 2007). The ability of mutations at R334 (at the outer mouth of the pore) to influence block by intracellular suramin (at the cytoplasmic entrance to the pore) (Fig. 6) therefore seems inconsistent with a direct interaction. The similar effects of mutations on block by intracellular suramin and intracellular $Pt(NO_2)_4^{2-}$ – in particular, the strong effects of R334C and R334E on the inhibitory effects of both blockers – suggest that these mutations affect suramin block and $Pt(NO_2)_4^{2-}$ block by a common mechanism. We propose that mutations at R334 alter block

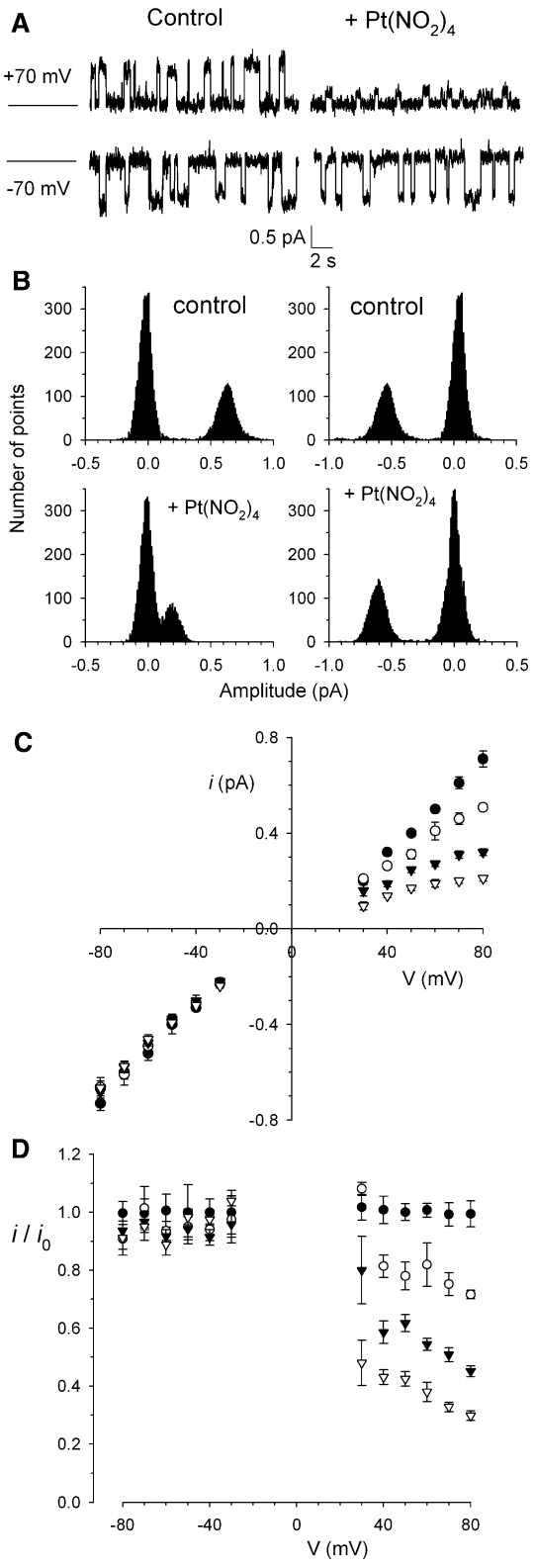

◀ **Fig. 9** Block of unitary currents by extracellular $Pt(NO_2)_4^{2-}$ ions. **a** Example single-channel currents recorded from inside-out patches at membrane potentials of +70 and –70 m*V*, as indicated. In each case the closed state of the channel is indicated by the *line on the far left*. Currents were recorded in the absence of $Pt(NO_2)_4^{2-}$ (Control) or with 10 mM $Pt(NO_2)_4^{2-}$ present in the extracellular solution (+ $Pt[NO_2]_4$). **b** Amplitude histograms prepared from these patches under the conditions shown in **a** at +70 m*V* (*left*) and –70 m*V* (*right*). **c** Mean unitary current-voltage relationships recorded in the absence of $Pt(NO_2)_4^{2-}$ (●) and with 1 mM (◯), 3 mM (▼) or 10 mM (▽) $Pt(NO_2)_4^{2-}$ present in the extracellular solution. **d** Mean fraction of control current remaining in the presence of different concentrations of extracellular $Pt(NO_2)_4^{2-}$ at different membrane potentials. Same symbols used as in **c**. Fractional current was significantly reduced by 10 mM $Pt(NO_2)_4^{2-}$ at all voltages between +30 and +80 m*V* and significantly reduced by both 1 and 3 mM $Pt(NO_2)_4^{2-}$ at all voltages between +40 and +80 m*V* ($p < 0.05$). Mean of data from three to six patches in **c** and **d**

by intracellular anions such as suramin and $Pt(NO_2)_4^{2-}$ that bind within the pore inner vestibule by an indirect mechanism. This suggests that mutations at R334 have far-reaching effects on pore structure and function, perhaps changing the conformation of the pore inner vestibule such that anion binding in the region of K95 and/or R303 is disrupted. However, we note that mutation of R334 has other effects on intracellular anion binding that are not replicated by mutation of either K95 or R303. Thus, all R334 mutants studied disrupted the dependence of intracellular $Pt(NO_2)_4^{2-}$ block on extracellular Cl^- ions (Fig. 5), whereas $Pt(NO_2)_4^{2-}$ block of both K95Q and R303Q remained Cl^-dependent (Figs. 1, 2). This suggests that the effects of mutation of R334 on the structure of the pore inner vestibule are not limited simply to the disruption of localized anion interactions with the pore.

Mutagenesis of R334 also alters current inhibition by external $Pt(NO_2)_4^{2-}$ ions (Figs. 10, 11). In wild-type CFTR, extracellular $Pt(NO_2)_4^{2-}$ causes a strongly voltage-dependent inhibition (Fig. 9) with an apparent K_d of ~2.8 mM at +80 m*V* (Fig. 10d); this may reflect voltage-dependent open channel block or surface charge screening. Because of the low single-channel conductance of R334-mutated forms of CFTR (Gong & Linsdell, 2004), it was not possible to investigate $Pt(NO_2)_4^{2-}$ block of these mutants directly by single-channel recording. Nevertheless, quantitative analysis of macroscopic current-voltage relationship rectification (Figs. 10, 11) suggests that block by external $Pt(NO_2)_4^{2-}$ was significantly weakened in all R334 mutants studied. In fact, all mutations that either removed or reversed the positive charge present at position 334 resulted in channels that were not significantly affected by the presence of 10 mM $Pt(NO_2)_4^{2-}$ in the extracellular solution according to this analysis (Fig. 11d). In contrast, the charge-conservative R334K mutant showed only very slightly weakened block by external $Pt(NO_2)_4^{2-}$ (Fig. 11d). Thus, current inhibition by external $Pt(NO_2)_4^{2-}$ ions shows very strong dependence on the presence of a positively charged side chain at this location in the outer mouth of the pore. This could be consistent with an open channel block mechanism, with R334 contributing to a binding site at which $Pt(NO_2)_4^{2-}$ occludes the channel pore or with a

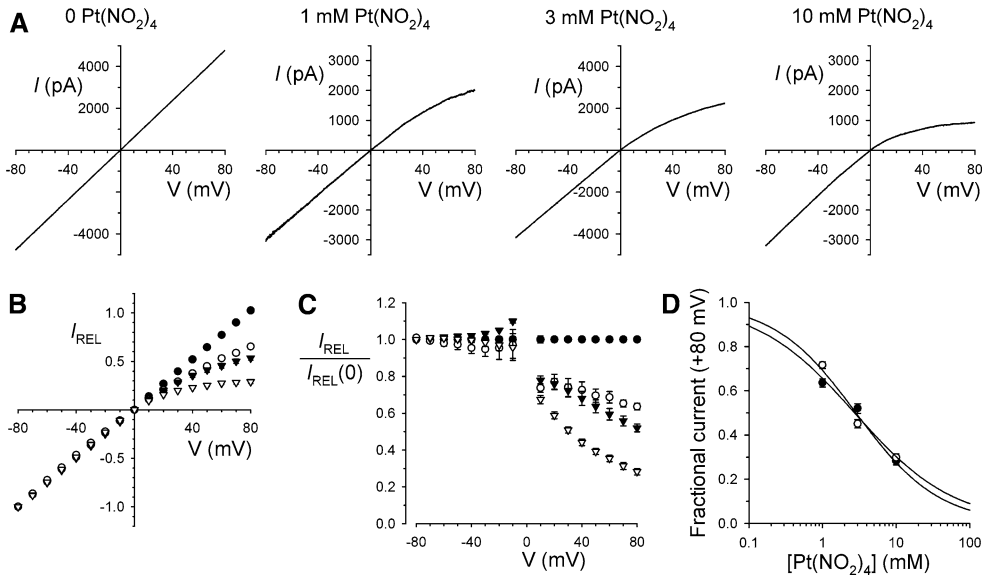

Fig. 10 Macroscopic current-voltage relationship shape reveals voltage-dependent inhibition by extracellular $Pt(NO_2)_4^{2-}$. **a** Example leak-subtracted macroscopic current-voltage relationships recorded without $Pt(NO_2)_4^{2-}$ or with 1, 3 or 10 mM $Pt(NO_2)_4^{2-}$ present in the extracellular solution as indicated. **b** Normalized current-voltage relationships illustrating the change in current rectification induced by $Pt(NO_2)_4^{2-}$ in the extracellular solution, for currents recorded in the absence of $Pt(NO_2)_4^{2-}$ (●) and with 1 mM (◯), 3 mM (▼) or 10 mM (▽) $Pt(NO_2)_4^{2-}$ present in the extracellular solution. Current amplitudes are shown relative to those at −80 m*V* (I_{REL}), as described in Methods. **c** Mean fraction of control normalized current remaining in the presence of different concentrations of extracellular $Pt(NO_2)_4^{2-}$ at different membrane potentials. Same symbols used as in **b**. Fractional relative current was significantly reduced by 1, 3 and 10 mM $Pt(NO_2)_4^{2-}$ at all voltages between +20 and +80 m*V* ($p < 0.001$). Mean of data from three to five patches in **b** and **c**. **d** Concentration dependence of inhibition by extracellular $Pt(NO_2)_4^{2-}$ estimated at +80 m*V*. Points represent data from single-channel experiments (◯, taken from Fig. 9d) or macroscopic current experiments (●, taken from Fig. 10c). Both sets of data have been fitted by equation 3, giving a K_d of 2.85 mM and n_H of 0.64 for single-channel currents and a K_d of 2.73 mM and n_H of 0.77 for macroscopic currents

charge screening mechanism whereby $Pt(NO_2)_4^{2-}$ screens the known electrostatic attractive effect of R334 on extracellular Cl^- ions (Smith et al., 2001). In contrast, neutralization of positive charges in the putative pore inner vestibule (K95, R303) had only very minor effects on block by external $Pt(NO_2)_4^{2-}$ ions (Fig. 11c,d), consistent with the critical factor for $Pt(NO_2)_4^{2-}$ inhibition being the presence of a positive charge at position 334. While mutation of R334 has previously been associated with a range of functional effects in CFTR (*see* Introduction), only current-voltage relationship rectification – likely reflecting electrostatic attraction of extracellular Cl^- ions into the outer mouth of the pore – has previously been strongly associated with amino acid side chain charge at this position (Smith et al., 2001; Gong & Linsdell, 2003a, 2004). Our present results are therefore consistent with a direct electrostatic interaction between extracellular $Pt(NO_2)_4^{2-}$ anions and the positive charge of the R334 side chain being critical for $Pt(NO_2)_4^{2-}$ binding in the outer mouth of the pore, leading to occlusion of the open channel and block of Cl^- permeation. Our results are also entirely consistent with extracellular $Pt(NO_2)_4^{2-}$ ions screening the surface charge contributed by R334 (or by the substituted lysine in R334K), resulting in loss of electrostatic attractive forces on extracellular Cl^- ions and reduced Cl^- entry into the pore at depolarized voltages. In this respect, we note that extracellular $Pt(NO_2)_4^{2-}$ ions, which block current only at depolarized voltages, do not reproduce the effect of charge-neutralizing mutations at R334, which cause a large decrease in single-channel conductance at all voltages (Gong & Linsdell, 2004). Irrespective of the exact mechanism of the interaction, the different dependence on side chain charge demonstrates that intracellular and extracellular $Pt(NO_2)_4^{2-}$ do not share a common interaction with R334.

Extracellular $Pt(NO_2)_4^{2-}$ ions also affect blocker interactions with the pore inner vestibule, an effect that we have previously suggested results from external $Pt(NO_2)_4^{2-}$ binding to a site outside the pore (Ge & Linsdell, 2006). The resulting negative interaction between external and internal $Pt(NO_2)_4^{2-}$ ions is apparently unaffected by a mutation that removes the positive charge associated with R334 (Fig. 8), even though all mutations affecting R334 interfere with the interaction between extracellular Cl^- ions and intracellular $Pt(NO_2)_4^{2-}$ ions (Fig. 5, *see below*). This result is consistent with the binding site for external $Pt(NO_2)_4^{2-}$ ions that leads to interactions with internal blockers (R334-independent) being distinct from the site with which external $Pt(NO_2)_4^{2-}$ ions interact to inhibit Cl^- permeation (R334-dependent) and supports the notion that

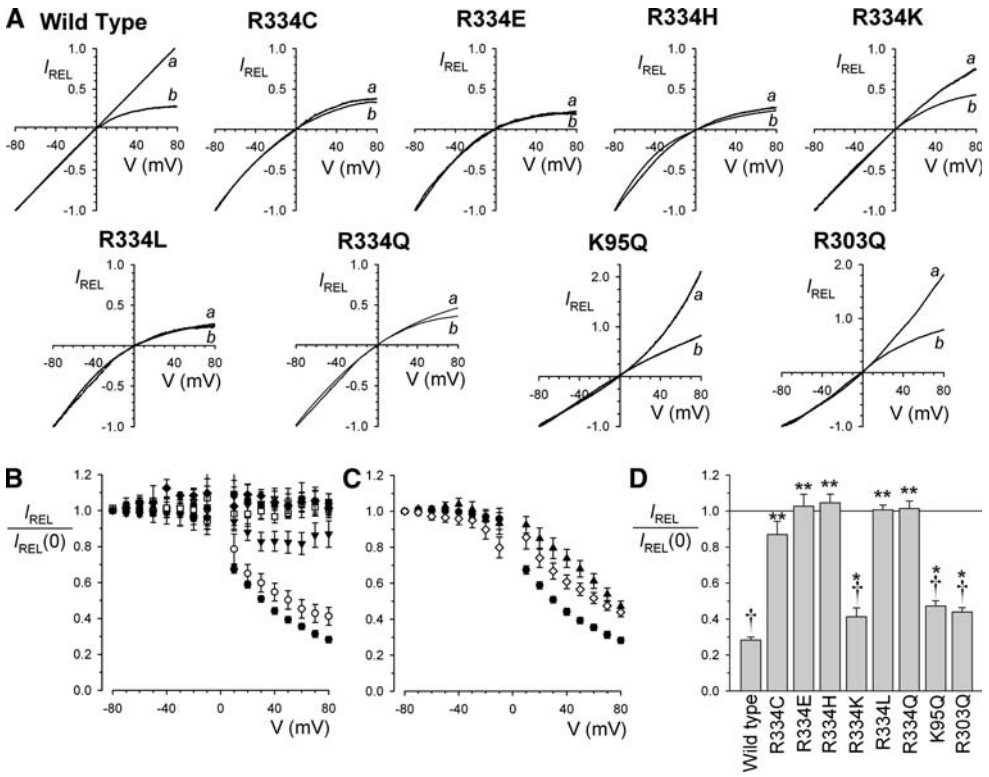

Fig. 11 Extracellular $Pt(NO_2)_4^{2-}$ block of pore mutants. **a** Example normalized, leak-subtracted macroscopic current-voltage relationships recorded without $Pt(NO_2)_4^{2-}$ (**a**) and with 10 mM $Pt(NO_2)_4^{2-}$ present in the extracellular solution (**b**) for different channel variants. Note the change in current rectification induced by extracellular $Pt(NO_2)_4^{2-}$ in wild type, R334K, K95Q and R303Q but not other R334 mutants. **b,c** Mean fraction of control normalized current remaining in the presence of 10 mM extracellular $Pt(NO_2)_4^{2-}$ at different membrane potentials for different channel variants: **b** wild type (●), R334C (▼), R334E (▽), R334H (■), R334K (◯), R334L (□), R334Q (◆); **c** wild type (●), K95Q (▲), R303Q (◇). **d** Normalized current remaining at +80 m*V* for different channel variants. Asterisks indicate a statistically significant difference from wild type ($*p < 0.05$, $**p < 0.0005$), while daggers indicate a significant difference from the same channel variant in the absence of $Pt(NO_2)_4^{2-}$ ($^{\dagger}p < 0.001$). Mean of data from three to six patches in **b–d**

the first site exists outside of the pore. Furthermore, we suggest that external $Pt(NO_2)_4^{2-}$ and external Cl^- destabilize the binding of internal blockers by different mechanisms since the effects of Cl^-, but not $Pt(NO_2)_4^{2-}$, are lost in R334Q. Thus, while extracellular $Pt(NO_2)_4^{2-}$ and mutagenesis of R334 both appear to have long-range effects on the conformation of the pore inner vestibule, these effects appear to be independent of each other.

We conclude that the multiple effects that are associated with mutagenesis of R334 in the outer mouth of the CFTR pore reflect both direct effects (interaction with anions at the outer mouth of the pore) and indirect effects (resulting from conformational changes occurring at a distance from the site of the mutation). Direct effects include loss of electrostatic attraction of permeant and impermeant ions from the extracellular solution to the outer mouth of the pore. As a result, these direct effects show a strong dependence on side chain charge, being strongly disrupted in all mutants except R334K. Indirect effects include weakened binding of intracellular blockers in the pore inner vestibule (Figs. 5, 7), loss of interactions between external Cl^- ions and intracellular blocking anions (Fig. 5c) (Gong & Linsdell, 2003a) and reduced single-channel conductance at hyperpolarized voltages (Gong & Linsdell, 2004). These indirect effects are relatively non-specific, occurring to some extent with all mutations. However, disruption of the effects of intracellular blockers is particularly pronounced in R334C and R334E (Figs. 5, 7). Currently, we have no explanation as to why R334C and R334E have so much more dramatic effects on block by intracellular $Pt(NO_2)_4^{2-}$ and suramin than other R334 mutations. Certainly, in the absence of direct structural information on the CFTR pore, it is impossible to predict how mutations at one site may be propagated over distance. One possibility consistent with our results would be that there is a component of pore structure that is absolutely dependent on the presence of an arginine residue at position 334 (which is disrupted in all mutants) and a separate structural alteration that occurs when an amino acid side chain containing a full (glutamate) or partial (cysteine)

negative charge is introduced at this position. Nevertheless, it also appears that some aspects of pore function are affected by mutation of R334 in an even more nonspecific way. Thus, the ability of extracellular Cl^- ions to destabilize block by intracellular $Pt(NO_2)_4^{2-}$ ions is practically abolished in all R334 mutants studied (Fig. 5c), suggesting that this interaction absolutely requires the presence of an arginine side chain in the outer pore mouth.

Previously, we suggested that interactions between extracellular Cl^- and intracellular anionic blockers might reflect ion-ion repulsion inside the channel pore that was dependent on the ability of the R334 side chain to coordinate the binding of multiple anions in the pore (Gong & Linsdell, 2003a). We believe that our present results point to an alternative explanation – namely, that mutation of R334 leads to a wide-ranging alteration in the architecture of the pore inner vestibule that disrupts ion-ion interactions. Since we also previously suggested that loss of these ion-ion interactions results in the low unitary conductance of R334-mutated forms of CFTR (Gong & Linsdell, 2004), it also seems likely that the reduced conductance of these mutants reflects, at least in part, structural effects that are propagated some distance from the location of R334 itself.

In summary, we propose that R334 contributes directly to electrostatic attraction of external anions and that mutations at this site also affect pore functional properties indirectly by changing the properties of other, distinct binding sites for internal anions.

Acknowledgements This work was supported by the Canadian Institutes of Health Research. We thank Elizabeth VandenBerg for technical assistance and Dr. Elizabeth Cowley for comments on the manuscript.

References

Cheung M, Akabas MH (1996) Identification of cystic fibrosis transmembrane conductance regulator channel-lining residues in and flanking the M6 membrane-spanning segment. Biophys J 70:2688–2695

Fatehi M, St Aubin CN, Linsdell P (2007) On the origin of asymmetric interactions between permeant anions and the CFTR chloride channel pore. Biophys J 92:1241–1253

Ge N, Linsdell P (2006) Interactions between impermeant blocking ions in the cystic fibrosis transmembrane conductance regulator chloride channel pore: evidence for anion-induced conformational changes. J Membr Biol 210:31–42

Ge N, Muise CN, Gong X, Linsdell P (2004) Direct comparison of the functional roles played by different transmembrane regions in the cystic fibrosis transmembrane conductance regulator chloride channel pore. J Biol Chem 279:55283–55289

Gong X, Burbridge SM, Cowley EA, Linsdell P (2002a) Molecular determinants of Au(CN)2− binding and permeability within the cystic fibrosis transmembrane conductance regulator Cl– channel pore. J Physiol 540:39–47

Gong X, Burbridge SM, Lewis AC, Wong PYD, Linsdell P (2002b) Mechanism of lonidamine inhibition of the CFTR chloride channel. Br J Pharmacol 137:928–936

Gong X, Linsdell P (2003a) Molecular determinants and role of an anion binding site in the external mouth of the CFTR chloride channel pore. J Physiol 549:387–397

Gong X, Linsdell P (2003b) Mutation-induced blocker permeability and multiion block of the CFTR chloride channel pore. J Gen Physiol 122:673–687

Gong X, Linsdell P (2004) Maximization of the rate of chloride conduction in the CFTR channel pore by ion-ion interactions. Arch Biochem Biophys 426:78–82

Green WN, Andersen OS (1991) Surface charges and ion channel function. Annu Rev Physiol 53:341–359

Kidd JF, Kogan I, Bear CE (2004) Molecular basis for the chloride channel activity of cystic fibrosis transmembrane conductance regulator and the consequences of disease-causing mutations. Curr Top Dev Biol 60:215–249

Lewis HA, Buchanan SG, Burley SK, Conners K, Dickey M, Dorwart M, Fowler R, Gao X, Guggino WB, Hendrickson WA, Hunt JF, Kearins MC, Lorimer D, Maloney PC, Post KW, Rajashankar KR, Rutter ME, Sauder JM, Shriver S, Thibodeau PH, Thomas PJ, Zhang M, Zhao X, Emtage S (2004) Structure of nucleotide-binding domain 1 of the cystic fibrosis transmembrane conductance regulator. EMBO J 23:282–293

Linsdell P (2005) Location of a common inhibitor binding site in the cytoplasmic vestibule of the cystic fibrosis transmembrane conductance regulator chloride channel pore. J Biol Chem 280:8945–8950

Linsdell P (2006) Mechanism of chloride permeation in the cystic fibrosis transmembrane conductance regulator chloride channel. Exp Physiol 91:123–129

Linsdell P, Hanrahan JW (1996) Disulphonic stilbene block of cystic fibrosis transmembrane conductance regulator Cl^- channels expressed in a mammalian cell line and its regulation by a critical pore residue. J Physiol 496:687–693

Linsdell P, Hanrahan JW (1998) Adenosine triphosphate-dependent asymmetry of anion permeation in the cystic fibrosis transmembrane conductance regulator chloride channel. J Gen Physiol 111:601–614

Liu X, Smith SS, Dawson DC (2003) CFTR: what's it like inside the pore? J Exp Zool 300A:69–75

Rosenberg MF, Kamis AB, Aleksandrov LA, Ford RC, Riordan JR (2004) Purification and crystallization of the cystic fibrosis transmembrane conductance regulator (CFTR). J Biol Chem 279:39051–39057

Sheppard DN, Welsh MJ (1999) Structure and function of the CFTR chloride channel. Physiol Rev 79:S23–S45

Smith SS, Liu X, Zhang Z-R, Sun F, Kriewall TE, McCarty NA, Dawson DC (2001) CFTR: covalent and noncovalent modification suggests a role for fixed charges in anion conduction. J Gen Physiol 118:407–431

St Aubin CN, Linsdell P (2006) Positive charges at the intracellular mouth of the pore regulate anion conduction in the CFTR chloride channel. J Gen Physiol 128:535–545

St Aubin CN, Zhou J-J, Linsdell P (2007) Identification of a second blocker binding site at the cytoplasmic mouth of the CFTR chloride channel pore. Mol Pharmacol 71:1360–1368

Woodull AM (1973) Ionic blockage of sodium channels in nerve. J Gen Physiol 61:687–708

Zhang Z-R, Song B, McCarty NA (2005) State-dependent chemical reactivity of an engineered cysteine reveals conformational changes in the outer vestibule of the cystic fibrosis transmembrane conductance regulator. J Biol Chem 280:41997–42003